JACS
JOURNAL OF THE AMERICAN CHEMICAL SOCIETY
Article
pubs.acs.org/JACS

Site-Specific Antibody–Polymer Conjugates for siRNA Delivery

Hua Lu,[†,∥] Danling Wang,[‡,∥] Stephanie Kazane,[‡] Tsotne Javahishvili,[§] Feng Tian,[§] Frank Song,[§] Aaron Sellers,[§] Barney Barnett,[§] and Peter G. Schultz*[,†,‡]

[†]Department of Chemistry, The Scripps Research Institute, La Jolla, California 92037, United States
[‡]California Institute for Biomedical Research, La Jolla, California 92037, United States
[§]Ambrx Inc., La Jolla, California 92037, United States

Supporting Information

ABSTRACT: We describe here the development of site-specific antibody–polymer conjugates (APCs) for the selective delivery of small interference RNAs (siRNAs) to target cells. APCs were synthesized in good yields by conjugating an aminooxy-derivatized cationic block copolymer to an anti-HER2 Fab or full-length IgG by means of genetically encoded *p*-acetyl phenylalanine (*p*AcF). The APCs all showed binding affinity comparable to that of HER2 as their native counterparts and no significant cellular cytotoxicity. Mutant S202-*p*AcF Fab and Q389-*p*AcF IgG polymer conjugates specifically delivered siRNAs to HER2$^+$ cells and mediated potent gene silencing at both the mRNA and protein levels. However, a mutant A121-*p*AcF IgG polymer conjugate, despite its high binding affinity to HER2 antigen, did not induce a significant RNA interference response in HER2$^+$ cells, presumably due to steric interference with antigen binding and internalization. These results highlight the importance of conjugation site on the activity of antibody–polymer-based therapeutics and suggest that such chemically defined APCs may afford a useful targeted delivery platform for siRNAs or other nucleic acid-based therapies.

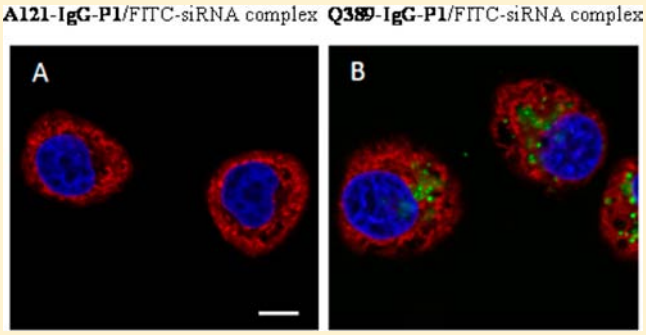

1. INTRODUCTION

The selective silencing of gene expression by small interference RNA (siRNA) is a promising approach for the treatment of a variety of human diseases, including cancer and metabolic, neurodegenerative, and infectious diseases.[1] However, a major obstacle to the clinical application of RNA interference (RNAi) therapy is the lack of efficient methods for the delivery of siRNAs to the target cells.[1g] To improve selective cellular uptake, decrease the overall dosage of siRNAs required for effective RNAi, and minimize off-target silencing in other tissues, a tissue-specific delivery system is highly desired.[2] To this end, a number of ligands that selectively bind tissue-associated antigens have been explored for targeted siRNA delivery, including a ScFv-9R conjugate,[3] antibody–protamine fusion proteins,[4] aptamer–siRNA chimeras,[5] cholesterol and folate–siRNA conjugates,[6,7] and a CpG oligonucleotide–siRNA conjugate.[8] However, these systems in general suffer from problems such as siRNA degradation, toll-like receptor 7-mediated immune responses, off-target gene silencing, and cytotoxicity. Various nanostructures coated with targeting ligands[9] including, for example, a leukocyte-targeted lipid nanoparticle coated with anti-β7 integrin antibody,[9j] have also been exploited for the selective delivery of siRNAs. However, conjugation of ligands such as antibodies to the surfaces of these nanostructures using conventional nonselective electrophilic conjugation chemistry generally leads to low ligand density, decreased binding affinity, and increased heterogeneity of the final materials.

In contrast to siRNAs, small-molecule toxins can be efficiently delivered to tumor cells as antibody conjugates and have demonstrated impressive efficacy in the clinic (e.g., Adcetris and Kadcyla). Moreover, it has recently been shown that the site-specific conjugation of drugs to antibodies can result in improved efficacy, pharmacokinetics, and therapeutic index relative to conventional nonspecific antibody conjugates.[10] One method for generating site-specific antibody conjugates involves the genetic incorporation of unnatural amino acids (UAAs)[11] into antibodies whose chemical reactivity is orthogonal to the 20 canonical amino acids. Specifically, a ketone-containing UAA, *p*-acetyl L-phenylalanine[12] (*p*AcF, Figure 1A), is genetically incorporated into the antibody at selected sites in response to the amber TAG codon using an evolved orthogonal tRNA/aminoacyl-tRNA synthetase pair specific for *p*AcF. The ketone group of *p*AcF can be selectively coupled to aminooxy-derivatized ligands by formation of a stable oxime bond under mild reaction conditions. Indeed, several site-specific antibody conjugates armed with various effector functions have been efficiently

Received: June 18, 2013
Published: August 7, 2013

   dx.doi.org/10.1021/ja4059525 | J. Am. Chem. Soc. 2013, 135, 13885–13891

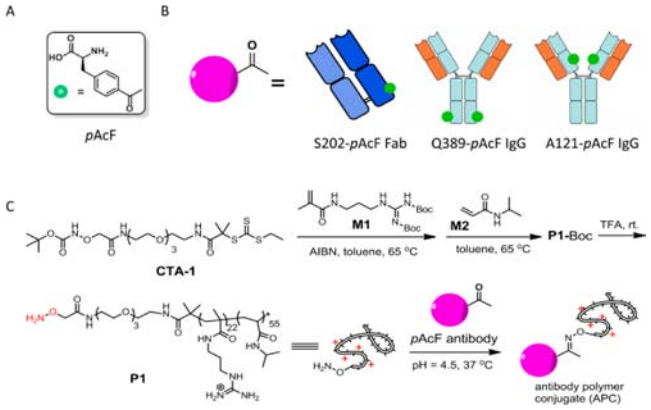

Figure 1. (A) Structure of *p*AcF. (B) Schematic illustration of *p*AcF-mutated anti-HER2 antibodies, S202-*p*AcF Fab, Q389-*p*AcF IgG, and A121-*p*AcF IgG. (C) Synthetic scheme for the antibody–polymer conjugates.

synthesized[13] by this method and have shown potent and selective *in vitro* and *in vivo* activity against tumor cells.

On the basis of the above studies, we reasoned that the site-specific conjugation of cationic polymers to antibodies which bind selectively to tumor-associated antigens and are efficiently internalized might potentially provide a targeted siRNA delivery system. In this case, the cationic polymer acts both to reversibly bind the siRNA and to facilitate the release of the payload from the endosomal/lysosomal compartments in the cell. When combined with modern controlled polymerization technologies, these site-specific antibody–polymer conjugates (APCs) may offer advantages over more conventional targeted polymeric siRNA delivery systems in that they provide more homogeneous, chemically defined structures that can be optimized with respect to affinity and physical properties and, for pharmaceutics, efficacy and ease of formulation.

Here we describe the synthesis of three site-specific APCs (**S202-Fab-P1**, **Q389-IgG-P1**, and **A121-IgG-P1**) through the keto group of the coupling reaction between an aminooxy-tethered cationic polymer **P1** and the *p*AcF mutant anti-HER2 antibodies, S202-*p*AcF Fab, Q389-*p*AcF IgG, and A121-*p*AcF IgG (Figure 1B). Furthermore, we show that siRNA complexes of **S202-Fab-P1** and **Q389-IgG-P1** can be efficiently and selectively delivered to $HER2^+$ cancer cells without significant cellular cytotoxicity. Surprisingly, we observed that the site of conjugation (e.g., **Q389-IgG-P1** vs **A121-IgG-P1**) can have a very significant impact on the *in vitro* activity of the APC/siRNA complexes. This is the first example of a site-specific APC for targeted siRNA delivery and underscores the important effect of conjugation site on the biological activity of the APC/siRNA complexes.

2. RESULTS AND DISCUSSION

2.1. Synthesis and Characterizations of HER2-Fab-P1.

Trastuzumab (Herceptin), a humanized antibody used for the treatment of $HER2^+$ breast cancers, binds to the extracellular juxta-membrane domain of HER2, a member of the epidermal growth factor receptor family that is highly overexpressed in approximately one-third of breast cancers, and is rapidly internalized into tumor cells.[14] On the basis of the Herceptin crystal structure, three solvent-exposed residues (S202 on the light chain; A121 and Q389 on the heavy chain) of which showed minimal perturbation on antibody expression and binding affinity in previous studies, were selected for substitution by *p*AcF.[12a,15] To site-specifically incorporate *p*AcF into the anti-HER2 Fab fragment at position S202 on the light chain (S202-*p*AcF Fab), an orthogonal amber suppressor tRNA/aaRS pair, derived from the tyrosyl *Methanococcus jannaschii* pair and evolved to selectively incorporate *p*AcF,[15] was coexpressed with the anti-HER2 Fab gene containing a TAG codon at S202 on the light chain in the presence of *p*AcF. The yield of the mutant S202-*p*AcF Fab was ~2 mg/L when grown in shake flasks and >400 mg/L in high-density fermentors after periplasmic lysis and protein G purification. To generate an anti-HER2 IgG with *p*AcF substituted for A121 (A121-*p*AcF IgG) or Q389 (Q389-*p*AcF IgG) on the heavy chain, an amber codon was substituted in the full-length anti-Her2 IgG1 gene at either heavy-chain residue A121 (HC-A121X) or Q389 (HC-Q389X) (a His-tag was added at the *C*-terminus of the heavy chain separately for the Q389-*p*AcF IgG). The mutant A121-*p*AcF and Q389-*p*AcF IgGs were produced in suspension Chinese hamster ovary (CHO-K1) cells by transient transfection in yields of ~3 mg/L.

We next synthesized the cationic polymer **P1** with an aminooxy group at one terminus. **P1** contains a cationic domain, consisting of side-chain guanidinium groups, which has been shown to endow membrane-penetrating activity to polymers regardless of their backbones,[16] and a poly(*N*-isopropylacrylamide) (PNIPAAm) domain to modulate the overall hydrophobicity of **P1**. Briefly, we first synthesized **CTA-1** (Figure 1C) as a chain transfer agent (CTA) for reversible addition–fragmentation chain-transfer polymerization (RAFT) (Scheme S1). **CTA-1** contains a Boc-protected aminooxy group, which provides a reactive handle for conjugation with antibodies after deprotection. Successive polymerization of monomers **M1** and **M2** (Figure 1C) in the presence of **CTA-1** and AIBN yielded block copolymer **P1**-Boc. Gel permeation chromatography (GPC) showed the molecular weight (MW) and polydispersity index (PDI) of **P1**-Boc to be 11.2 kDa and 1.29, respectively (Figure S1). Deprotection of **P1**-Boc by TFA and subsequent extensive dialysis against ultrapure water yielded the highly water-soluble, cationic polymer **P1** bearing an aminooxy group. The MW of **P1** is ~10.1 kDa, and the average degree of polymerization (DP) of **M1** and **M2** are ~22 and 55, respectively, as determined by ^{1}H NMR spectroscopy (Figure S2). Overall, the MW of **P1** (determined by ^{1}H NMR) agreed well with the MW of its precursor **P1**-Boc (determined by GPC).

We next generated an APC (**S202-Fab-P1**) by incubating the S202-*p*AcF Fab (~5 mg/mL) and **P1** (~100 mg/mL) in 100 mM acetate buffer (pH 4.5) at 37 °C for 3–5 days. Purification by protein G and subsequent size exclusion chromatography removed unreacted starting materials and afforded the pure conjugate in about 60% yield. SDS-PAGE (Figure 2A) analysis of **S202-Fab-P1** showed a diffuse band from ~50 to 65 kDa under non-reducing conditions, indicating formation of the APC. Under reducing conditions (10 mM DTT), a discrete band at ~24 kDa and a diffuse band at ~26–42 kDa were observed for the APC, which correspond to the native heavy chain and the light chain–**P1** conjugate, respectively. An enzyme-linked immunosorbent assay (ELISA) showed **S202-Fab-P1** bound to HER2 antigen with affinity similar to that of S202-*p*AcF Fab (EC_{50} values of 0.6 ± 0.2 and 1.2 ± 0.3 nM, respectively) (Figure 2B), indicating that the binding of S202-*p*AcF Fab to antigen was not impaired by **P1** conjugation. The cationic **P1** of **S202-Fab-P1** should form a complex with the

dx.doi.org/10.1021/ja4059525 | J. Am. Chem. Soc. 2013, 135, 13885–13891

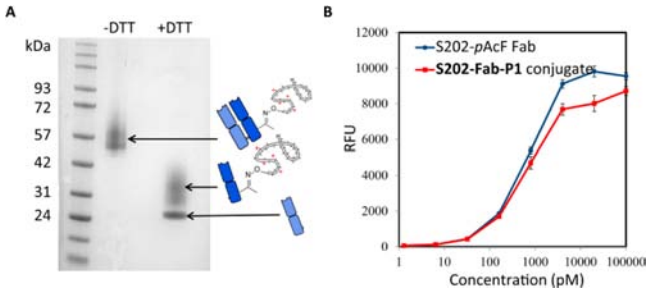

Figure 2. SDS-PAGE gel and ELISA assay of **S202-Fab-P1**. (A) **S202-Fab-P1** was analyzed by SDS-PAGE under both non-reducing (−DTT) and reducing (+DTT, 10 mM) conditions and stained with Coomassie brilliant blue. (B) ELISA assay of anti-HER2 S202-*p*AcF Fab and **S202-Fab-P1** binding to HER2 antigen. An anti-human Ig kappa chain−HRP conjugate was used as the secondary antibody, and binding affinity was assayed using fluoroscence by QuantaBlu Fluorogenic Peroxidase Substrate.

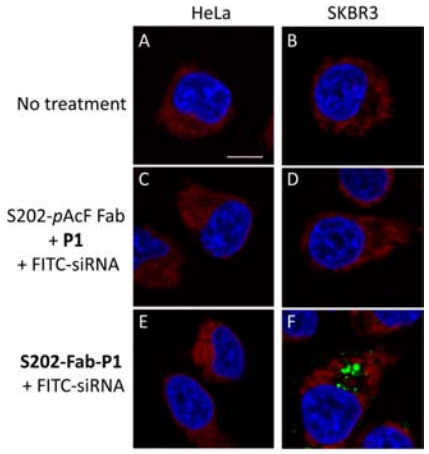

Figure 3. Confocal microscopy of internalization of siRNA mediated by **S202-Fab-P1**. HeLa (A,C,E) and SKBR-3 (B,D,F) cells were treated with buffer (A,B), 200 nM S202-*p*AcF Fab + 200 nM **P1** + 50 nM siRNA-FITC (C,D), or 200 nM **S202-Fab-P1** + 50 nM siRNA-FITC (E,F) for 4 h. Cells were then stained with Hoechst 33342 (blue) and ER-Tracker (red) and imaged with a Leica 710 confocal microscope. Bar = 10 μm.

negatively charged siRNAs. As expected, a gel retardation assay showed that **S202-Fab-P1** binds siRNA completely at molar ratio of 1.5/1 or higher after 1 min incubation at room temperature in PBS (pH 7.4) (Figure S3). Dynamic light scattering (DLS) further showed that a complex with average size about 50−60 nm formed when **S202-Fab-P1** and siRNA were mixed at a 2/1 molar ratio under the same conditions (Figure S4).

2.2. S202-Fab-P1 Selectively Delivers FITC-siRNA to HER2$^+$ Cells. To test the ability of **S202-Fab-P1** to selectively deliver siRNAs to the target cells, either the APC (200 nM) or a control mixture of anti-HER2 S202-*p*AcF Fab and **P1** (200 nM each) was mixed with FITC-siRNA (from Dharmacoml Thermo Scientific Inc., 50 nM) at room temperature and then added to SKBR-3 (HER2$^+$ human breast cancer) or HeLa (HER2$^-$ human cervical cancer) cell cultures. Four hours after treatment, cells were washed multiple times with cold PBS, labeled with Hoechst 33342 (blue) and ER-Tracker (red), and observed under a LSM 710 confocal microscope. Unlike the mixture of S202-*p*AcF Fab and **P1**, which showed non-detectable FITC fluorescence in both SKBR-3 and HeLa cells, **S202-Fab-P1** affords strong FITC fluorescence in HER2$^+$ positive SKBR-3 cells, but not in HER2$^-$ HeLa cells (Figure 3). Cell viability assays showed that treatment with complexes of **S202-Fab-P1**/scrambled-siRNA resulted in no obvious cytotoxicity at concentrations up to 300 nM/100 nM (Figure S5). These results indicate that **S202-Fab-P1** can effectively deliver siRNAs to the HER2$^+$ cells at concentrations where it is not toxic.

2.3. S202-Fab-P1/siRNA Complexes Selectively Knockdown Genes in HER2$^+$ Cells in a HER2-Dependent Manner. Next, we determined whether the siRNA delivered to the HER2$^+$ cells by **S202-Fab-P1** can selectively induce gene silencing. Various concentrations of **S202-Fab-P1** were mixed with 50 nM GAPDH-specific siRNA (GAPDH-siRNA) in serum-free Opti-MEM and then incubated with SKBR-3 cells at 37 °C for 4 h. Relative GAPDH mRNA levels (normalized to β-actin) were measured by quantitative real-time polymerase chain reaction (qRT-PCR) 24 h after treatment. As shown in Figure 4A, **S202-Fab-P1**/siRNA ratios of 100 nM/50 nM, 150 nM/50 nM, and 200 nM/50 nM induce a concentration-dependent silencing of GAPDH (blue bars, lanes 1−3), and a 300 nM/100 nM ratio of **S202-Fab-P1**/GAPDH-siRNA complex resulted in 88% knockdown of GAPDH mRNA (Figure 4A, blue bars, lane 4). In contrast, neither the complex of a scrambled-siRNA with **S202-Fab-P1** nor the GAPDH-siRNA delivered by the S202-*p*AcF Fab and **P1** mixture showed any significant silencing of mRNA expression (Figure 4A, blue bars, lanes 5 and 6). Moreover, treatment with the **S202-Fab-P1**/GAPDH-siRNA complex failed to induce gene silencing of GAPDH in HeLa (Figure 4A, greens bars) and NIH-3T3 (Figure 4A, red bars) cells, two HER2$^-$ cell lines. Additionally, this selectivity was well maintained at higher siRNA dosages by using relatively lower APC/siRNA ratios. To confirm gene silencing by the **S202-Fab-P1**/siRNA complex at the protein level, Western blot analysis was performed. Consistent with the qRT-PCR results, treatment with increased concentrations of the **S202-Fab-P1**/GAPDH-siRNA complex resulted in a dose-dependent decrease of GAPDH protein levels in SKBR-3 cells and was more efficient in gene silencing than commercial lipofectamine transfection at the same siRNA concentration (Figure 4B, top two lanes). Again, no significant reduction in GAPDH protein levels was observed for the **S202-Fab-P1**/GAPDH-siRNA complex at the same concentrations in HER2$^-$ HeLa cells (Figure 4B, bottom two lanes) and NIH-3T3 cells (Figure S6). We further confirmed that the gene silencing induced by the **S202-Fab-P1**/GFP-siRNA complex in SKBR-3 cells was HER2 dependent in a competition assay. When SKBR-3 cells were pretreated with 10 μM anti-HER2 IgG, GAPDH mRNA levels decreased only 30%, relative to an 85% reduction by the **S202-Fab-P1**/GFP-siRNA complex at 300 nM/100 nM in the absence of competing antibody (Figure 4C). Overall, these results indicate that the **S202-Fab-P1** conjugate can selectively deliver siRNA to HER2$^+$ cells and efficiently suppress expression of the targeted gene at both the mRNA and protein levels in a HER2-dependent manner.

To show that **S202-Fab-P1** is a general delivery vehicle for siRNAs to HER2$^+$ cells, we tested a number of other siRNAs against different targets. As shown in Figure S7, a dose-dependent (up to 72%) knockdown of MDM2 at both the mRNA and protein levels in SKBR-3 cells was observed when **S202-Fab-P1** (300 nM) was used to deliver a siRNA against MDM2 (MDM2-siRNA, 100 nM), a well-known negative

dx.doi.org/10.1021/ja4059525 | J. Am. Chem. Soc. 2013, 135, 13885−13891

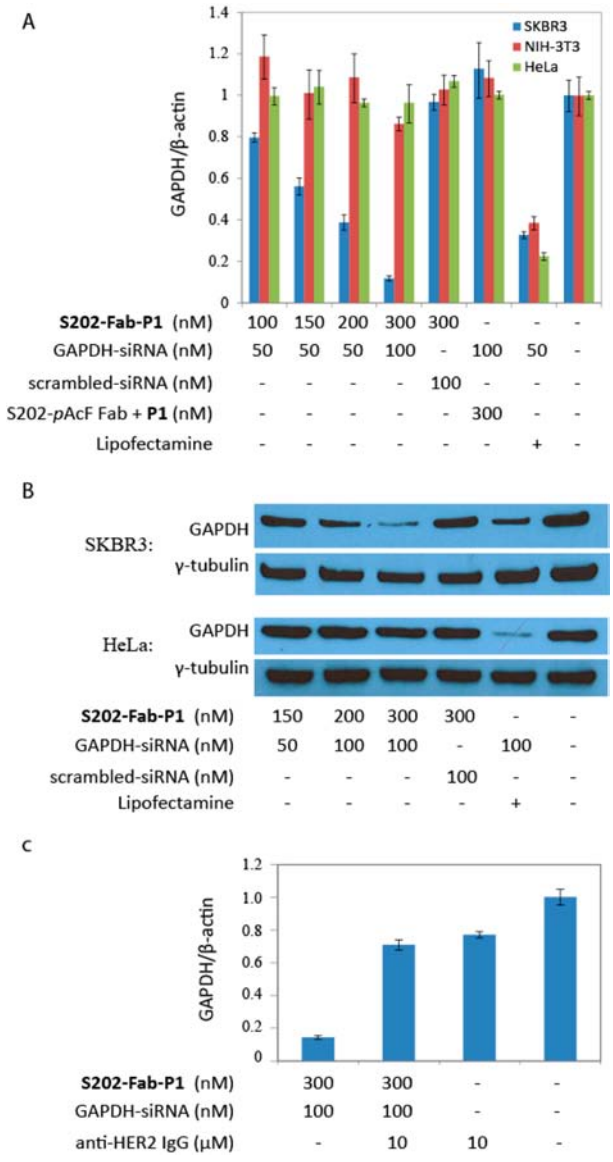

Figure 4. Cell-selective RNA silencing induced by the **S202-Fab-P1**/siRNA complexes. (A) CYBR-Green quantitative real-time PCR (qRT-PCR) analysis of the gene silencing at the mRNA level in $HER2^+$ and $HER2^-$ cells; the **S202-Fab-P1**/GAPDH-siRNA complexes reduce relative GAPDH mRNA levels in SKBR-3 (blue), but not NIH-3T3 (red) or HeLa (green) cells. Twenty-four hours after treatment, cells were lysed for qRT-PCR analysis; the relative expression levels of GAPDH mRNA were normalized to β-actin and compared with the untreated group. (B) Western blot analysis of gene silencing at the protein level in $HER2^+$ and $HER2^-$ cells; the **S202-Fab-P1**/GAPDH-siRNA complexes reduce protein levels of GAPDH in SKBR-3 but not HeLa cells. Seventy-two hours after treatment, cells were lysed and GAPDH levels were measured; γ-tubulin served as the internal control. (C) qRT-PCR analysis of gene silencing at the mRNA level in SKBR-3 cells for the HER2 competition study; the results showed that the RNA silencing by the **S202-Fab-P1**/siRNA complex in SKBR-3 is HER2-dependent; SKBR-3 cells were treated with 10 μM anti-HER2 IgG and incubated in Opti-MEM for 1 h before they were treated with the **S202-Fab-P1**/siRNA complex at 300 nM/100 nM; 4 h later, the medium was replaced with complete medium with 10% FBS for all the treatment groups; cells were harvested for qRT-PCR 24 h post treatment.

transcriptional regulator of the tumor suppressor protein p53. Up to 77% knockdown of DNAJB11 mRNA in SKBR-3 cells was also observed with the complex formed by **S202-Fab-P1** (300 nM) and a siRNA targeting DNAJB11 (DNAJB11-siRNA, 100 nM), a co-chaperon protein belonging to the DNAJ/HSP40 family (Figure S8). Additionally, no significant GFP silencing was observed in a stable 293T-GFP cell line ($HER2^-$) treated with the complex of **S202-Fab-P1** (300 nM) and a siRNA against GFP (GFP-siRNA, 100 nM) (Figure S9). Together, these results clearly demonstrate that **S202-Fab-P1** is able to selectively knockdown a variety of genes in $HER2^+$ cells.

2.4. APCs-Induced Gene Silencing Is Site-Dependent.

We next synthesized site-specific **P1** conjugates of the full-length anti-HER2 Q389-*p*AcF and A121-*p*AcF mutant IgGs to determine if higher binding affinity and bivalency lead to more potent mRNA silencing. Two conjugates, **Q389-IgG-P1** and **A121-IgG-P1**, were synthesized and purified as described above (Figures 1C and S12). ELISA analysis showed that the two conjugates have binding affinity similar to that of HER2 antigen, with IC_{50} values of 0.35 nM (**A121-IgG-P1**) and 0.87 nM (**Q389-IgG-P1**); these affinities are comparable to those of their parent antibody (Figure S13). Gel retardation assays showed complete siRNA binding by the two **IgG-P1** conjugates at an APC/siRNA molar ratio of ~0.4/1 (Figure S14); DLS analysis confirmed the formation of the complexes (Figure S15). Surprisingly, confocal microscopy showed that **A121-IgG-P1** (50 nM) failed to deliver FITC-siRNA (50 nM) to SKBR-3 cells (Figure 5A). Consistent with this result, the **A121-IgG-P1**/GAPDH-siRNA complex did not induce RNA silencing in SKBR-3 at concentrations as high as 300 nM/100 nM, as determined by qRT-PCR (Figure S16). In contrast, **Q389-IgG-P1** delivered the FITC-siRNA to SKBR-3 cells under the same conditions used for **A121-IgG-P1** (Figure 5B).

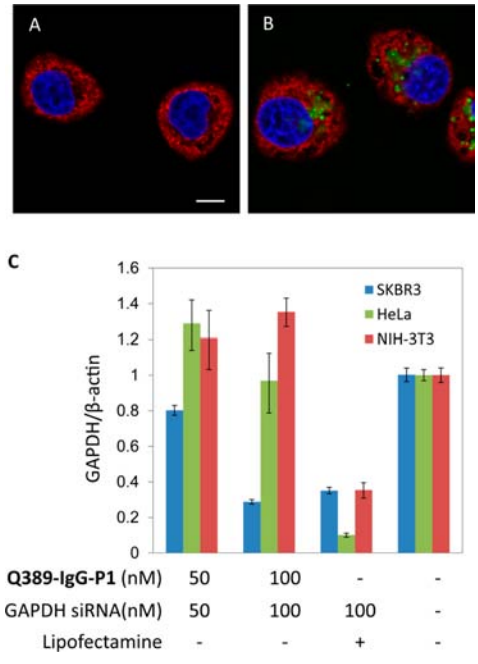

Figure 5. Site-dependent cell internalization and RNA silencing for **A121-IgG-P1** and **Q389-IgG-P1**. (A,B) Confocal microscopy of FITC-siRNA delivered to SKBR-3 cells by **A121-IgG-P1** (A) and **Q389-IgG-P1** (B). (C) CYBR-Green qRT-PCR analysis of gene silencing at the mRNA level in $HER2^+$ and $HER2^-$ cells; the results showed that the **Q389-IgG-P1**/GAPDH-siRNA complex reduces relative GAPDH mRNA levels in SKBR-3 (blue), but not NIH-3T3 (red) and HeLa (green) cells.

dx.doi.org/10.1021/ja4059525 | J. Am. Chem. Soc. 2013, 135, 13885−13891

Moreover, **Q389-IgG-P1** delivered the GAPDH-siRNA efficiently to SKBR-3 cells but not HeLa cells and NIH-3T3 cells, as determined by the selective mRNA silencing (Figure 5C) and protein knockdown (Figure S17). The RNA silencing effect of the **Q389-IgG-P1**/GAPDH-siRNA complex at 100 nM/100 nM was comparable to that of the **S202-Fab-P1**/GAPDH-siRNA at 300 nM/100 nM, indicating **Q389-IgG-P1** is more potent than **S202-Fab-P1**. Considering the conjugation site of **A121-IgG-P1** (CH1 region) is much closer to the antigen binding site than for **Q389-IgG-P1** (CH3 region), the difference in the efficacies of siRNA delivery by these two APCs is likely due to steric interference of the antigen binding site of **A121-IgG-P1** but not **Q389-IgG-P1** when the APC/siRNA complexes are formed.

3. CONCLUSIONS

We have demonstrated that site-specific APCs can be readily synthesized under mild conditions in good yields by the genetic incorporation of an UAA with bioorthogonal reactivity. These APCs have a high binding affinity to HER2 antigen that is comparable to that of their parent antibodies. **S202-Fab-P1** and **Q389-IgG-P1** effectively and selectively deliver functional siRNAs to $HER2^+$ cancer cells with no obvious toxicity. Significant gene silencing at both the mRNA and protein levels was observed using a number of different siRNAs. We also demonstrate that the conjugation site of the APCs plays a critical role in determining the efficient internalization and silencing of the APC/siRNA complexes. We are currently further optimizing the structure and MW of the polymer as well as testing siRNA delivery of these novel APCs *in vivo*. This site-specific APC platform may provide a novel approach for the selective delivery of siRNAs or other nucleic acid-based therapeutic agents.

4. EXPERIMENTAL SECTION

Synthesis of P1. **CTA-1** (12 mg, 0.02 mmol), **M1** (150 mg, 0.39 mmol), and AIBN (2 mg, 0.012 mmol) were added to a 25 mL two-neck round-bottom flask. Under argon, the mixture was dissolved in toluene (3 mL) and heated to 65 °C for 3 days; ^{1}H NMR indicated more than 95% **M1** was consumed. **M2** (NIPAAm, 90 mg, 0.8 mmol) was then added to the solution via syringe. The reaction was stirred under argon at 65 °C for another 2 days; ^{1}H NMR confirmed the consumption of both **M1** and **M2**. An aliquot (10 μL) of the **P1**-Boc solution was injected directly into the GPC for MW analysis (Figure S1), and the rest of the solution was dried under vacuum. The residual oil was dissolved in trifluoroacetic acid (TFA, 3 mL) and stirred at room temperature overnight to remove the Boc group. TFA was removed under vacuum, and the residue was dissolved in 5 mL of ultrapure water and extensively dialyzed against ultrapure water to remove any small molecular impurities. Water was changed every 4−6 h for a total of four times. The solution was then lyophilized to afford a white fluffy powder (126 mg, yield 73%). The ^{1}H NMR spectrum of **P1** is shown in Figure S2.

Mutation and Expression of the Anti-HER2 Q389-pAcF IgG. The herceptin gene containing a TAG codon at site Q389 (HC-Q389X) and a His-tag at the *C*-terminus of the heavy chain was amplified by PCR and inserted into a plasmid containing an orthogonal *Escherichia coli* tyrosyl-derived tRNA/aaRS pair that incorporates *p*AcF. The mutant Q389-*p*AcF IgG was expressed in a suspension of CHO cells using Free Style Max (Life Technologies, Carlsbad, CA) as a transfection reagent. For a 30 mL scale transfection, CHO cells were seeded at 0.5×10^6/mL the day before transfection. On the day of transfection, cells were counted before transfection to ensure a cell density of 1.0×10^6/mL. *p*AcF in PBS was added into cell culture flask 15 min before transfection (final concentration 1.3 mM). To two separate tubes each containing 0.6 mL of OptiPRO media were added 45 μg of the mutant pLou plasmid and 37.5 μL of MAX reagent separately. The MAX/OptiPRO solution was then added to the DNA/OptiPRO solution and mixed by swirling the tube gently. The complex was incubated for 15 min and then poured into 30 mL of the CHO cell culture. The flask was transferred to a 32 °C incubator shaking at 125 rpm. Three milliliters of 10× cell boost 5 (70 g/L stock solution; HyClone) was added to the cell culture 24 h after transfection; the medium was harvested 7 days after transfection by centrifugation. The supernatant was filtered with a 0.22 μM filter, and the mutant Q389-*p*AcF IgG was purified by Ni-NTA column (Qiagen, Valencia, CA) in a yield of ∼2.5−3 mg/L. The structure and molecular weight of the antibody were confirmed by SDS-PAGE gel (Figure S10) and ESI-MS (Figure S11).

Synthesis of S202-Fab-P1. The mutant S202-*p*AcF Fab was buffer exchanged to 100 mM acetate buffer (pH 4.5) and concentrated to ∼5 mg/mL with a 10 kDa Amicon concentrator before reaction. **P1** (18 mg, ∼1.8 μmol $-ONH_2$) was dissolved in 100 mM acetate buffer (pH 4.5, 50 μL) in a 0.5 mL Eppendorf tube. The S202-*p*AcF Fab (5.2 mg/mL, 200 μL) was slowly added to the **P1** solution. The mixture was incubated at 37 °C for ∼3−5 days and then quenched by slow addition to protein G column binding buffer (50 mM NaOAc, pH 5.2, 1.5 mL). The mixture was passed through a benchtop protein G column (to increase yield, repeat this for another three times). The column was washed extensively with binding buffer (∼100 mL) and eluted with protein G elution buffer (100 mM glycine, pH 3.0, 10 mL). The eluent was immediately neutralized with Tris·HCl buffer (1.0 M, pH 7.4, 1.0 mL) and concentrated with a 10 kDa Amicon concentrator to ∼0.5 mL. The conjugate was further purified by size exclusion chromatography (Superdex 200, 10/300 GL, GE healthcare) on a FPLC system using 1× dPBS as mobile phase. The desired fractions were combined and concentrated with a 10 kDa Amicon concentrator to give **S202-Fab-P1** (0.5 mg/mL of antibody × 1.2 mL, determined by both nanodrop absorption at 280 nm and BCA protein detection kit) in a yield of ∼60%. **Q389-IgG-P1** and **A121-IgG-P1** were synthesized following the same protocol; the yield of **Q389-IgG-P1** and **A121-IgG-P1** after purification averaged 40%. The conjugates were confirmed by SDS-PAGE (Figure S12).

Confocal Microscopy. SKBR-3 and HeLa cells were seeded separately in two 35 mm four-chamber glass-bottom dishes at 100 000 and 80 000 cells/well, respectively. The dishes were incubated at 37 °C for 24 h to reach 50−70% confluence. Before treatment, the complete medium was removed, and cells were washed with PBS once and incubated with 400 μL of Opti-MEM (Life Technologies, Carlsbad, CA). To make the **S202-Fab-P1**/FITC-siRNA complexes, **S202-Fab-P1** and FITC-siRNA were diluted to desired concentrations in 50 μL of Opti-MEM separately. Equal volumes of **S202-Fab-P1** and FITC-siRNA in Opti-MEM were mixed together and incubated at room temperature for 10−20 min. The control mixture of anti-HER2 S202-*p*AcF Fab, **P1**, and FITC-siRNA was prepared in the same way. The **S202-Fab-P1**/FITC-siRNA complex and the control mixture in 100 μL of Opti-MEM were added to SKBR-3 and HeLa cells and incubated at 37 °C for 4 h. Opti-MEM was removed, and cells were stained with ER tracker red (1/2000 dilution) and Hoechst (1/5000 dilution) in PBS (500 μL). After incubation at room temperature for 10 min, the medium was removed, and cells were washed with cold PBS multiple times and imaged.

siRNA Delivery. Cells were incubated in 24-well plates in DMEM supplied with 10% FBS until they reached 50−70% confluence. Complete medium was removed before treatment, and cells were washed with PBS and replaced with 400 μL of Opti-MEM (Life Technologies, Carlsbad, CA). To make the **S202-Fab-P1**/siRNA complexes, **S202-Fab-P1** and the appropriate siRNAs were diluted to the desired concentrations in 50 μL of Opti-MEM separately. Equal volumes of **S202-Fab-P1** and siRNA in Opti-MEM were mixed together and incubated at room temperature for 10−20 min. The **S202-Fab-P1**/siRNA complexes in 100 μL of Opti-MEM were then added to cells and incubated at 37 °C for 4 h. Positive controls were performed using Lipofectamine RNAi MAX (Life Technologies, Carlsbad, CA) following the manufacturer's protocol. The Opti-MEM medium was replaced by DMEM supplied with 10% FBS without

antibiotics 4 h after treatment. The cells were analyzed by either qRT-PCR (24−48 h post treatment) or Western blot (48−72 h post treatment) at appropriate time points.

■ ASSOCIATED CONTENT

Supporting Information

Additional experimental details and supplementary figures. This material is available free of charge via the Internet at http://pubs.acs.org.

■ AUTHOR INFORMATION

Corresponding Author

schultz@scripps.edu

Author Contributions

‖H.L. and D.W. contributed equally.

Notes

The authors declare no competing financial interest.

■ ACKNOWLEDGMENTS

This work is supported by NIH grant R01 GM062159. H.L. is The Jake Wetchler Foundation Fellow for Pediatric Innovation of the Damon Runyon Cancer Research Foundation (DRG-2099-11). We thank Dr. M.G. Finn and his group for use of their GPC and DLS facilities.

■ REFERENCES

(1) (a) Yu, D. B.; Pendergraff, H.; Liu, J.; Kordasiewicz, H. B.; Cleveland, D. W.; Swayze, E. E.; Lima, W. F.; Crooke, S. T.; Prakash, T. P.; Corey, D. R. *Cell* **2012**, *150*, 895−908. (b) Watts, J. K.; Corey, D. R. *J. Pathol.* **2012**, *226*, 365−379. (c) Lima, W. F.; Prakash, T. P.; Murray, H. M.; Kinberger, G. A.; Li, W. Y.; Chappell, A. E.; Li, C. S.; Murray, S. F.; Gaus, H.; Seth, P. P.; Swayze, E. E.; Crooke, S. T. *Cell* **2012**, *150*, 883−894. (d) Stanton, M. G.; Colletti, S. L. *J. Med. Chem.* **2010**, *53*, 7887−7901. (e) Davis, M. E.; Zuckerman, J. E.; Choi, C. H. J.; Seligson, D.; Tolcher, A.; Alabi, C. A.; Yen, Y.; Heidel, J. D.; Ribas, A. *Nature* **2010**, *464*, 1067−1070. (f) Bennett, C. F.; Swayze, E. E. *Annu. Rev. Pharmacol.* **2010**, *50*, 259−293. (g) Whitehead, K. A.; Langer, R.; Anderson, D. G. *Nat. Rev. Drug Discov.* **2009**, *8*, 129−138. (h) Jeong, J. H.; Mok, H.; Oh, Y. K.; Park, T. G. *Bioconjugate Chem.* **2009**, *20*, 5−14. (i) Zimmermann, T. S.; Lee, A. C. H.; Akinc, A.; Bramlage, B.; Bumcrot, D.; Fedoruk, M. N.; Harborth, J.; Heyes, J. A.; Jeffs, L. B.; John, M.; Judge, A. D.; Lam, K.; McClintock, K.; Nechev, L. V.; Palmer, L. R.; Racie, T.; Rohl, I.; Seiffert, S.; Shanmugam, S.; Sood, V.; Soutschek, J.; Toudjarska, I.; Wheat, A. J.; Yaworski, E.; Zedalis, W.; Koteliansky, V.; Manoharan, M.; Vornlocher, H. P.; MacLachlan, I. *Nature* **2006**, *441*, 111−114.

(2) (a) Zhou, J. H.; Rossi, J. J. *Oligonucleotides* **2011**, *21*, 1−10. (b) Peer, D.; Lieberman, J. *Gene Ther.* **2011**, *18*, 1127−1133.

(3) Kumar, P.; Ban, H. S.; Kim, S. S.; Wu, H. Q.; Pearson, T.; Greiner, D. L.; Laouar, A.; Yao, J. H.; Haridas, V.; Habiro, K.; Yang, Y. G.; Jeong, J. H.; Lee, K. Y.; Kim, Y. H.; Kim, S. W.; Peipp, M.; Fey, G. H.; Manjunath, N.; Shultz, L. D.; Lee, S. K.; Shankar, P. *Cell* **2008**, *134*, 577−586.

(4) (a) Yao, Y. D.; Sun, T. M.; Huang, S. Y.; Dou, S.; Lin, L.; Chen, J. N.; Ruan, J. B.; Mao, C. Q.; Yu, F. Y.; Zeng, M. S.; Zang, J. Y.; Liu, Q.; Su, F. X.; Zhang, P.; Lieberman, J.; Wang, J.; Song, E. W. *Sci. Transl. Med.* **2012**, *4*, 130ra48. (b) Song, E. W.; Zhu, P. C.; Lee, S. K.; Chowdhury, D.; Kussman, S.; Dykxhoorn, D. M.; Feng, Y.; Palliser, D.; Weiner, D. B.; Shankar, P.; Marasco, W. A.; Lieberman, J. *Nat. Biotechnol.* **2005**, *23*, 709−717. (c) Peer, D.; Zhu, P. C.; Carman, C. V.; Lieberman, J.; Shimaoka, M. *Proc. Natl. Acad. Sci. U.S.A.* **2007**, *104*, 4095−4100.

(5) (a) Thiel, K. W.; Hernandez, L. I.; Dassie, J. P.; Thiel, W. H.; Liu, X.; Stockdale, K. R.; Rothman, A. M.; Hernandez, F. J.; McNamara, J. O.; Giangrande, P. H. *Nucleic Acids Res.* **2012**, *40*, 6319−6337. (b) Dassie, J. P.; Liu, X. Y.; Thomas, G. S.; Whitaker, R. M.; Thiel, K. W.; Stockdale, K. R.; Meyerholz, D. K.; McCaffrey, A. P.; McNamara, J. O.; Giangrande, P. H. *Nat. Biotechnol.* **2009**, *27*, 839−849. (c) McNamara, J. O.; Andrechek, E. R.; Wang, Y.; D Viles, K.; Rempel, R. E.; Gilboa, E.; Sullenger, B. A.; Giangrande, P. H. *Nat. Biotechnol.* **2006**, *24*, 1005−1015.

(6) Wolfrum, C.; Shi, S.; Jayaprakash, K. N.; Jayaraman, M.; Wang, G.; Pandey, R. K.; Rajeev, K. G.; Nakayama, T.; Charrise, K.; Ndungo, E. M.; Zimmermann, T.; Koteliansky, V.; Manoharan, M.; Stoffel, M. *Nat. Biotechnol.* **2007**, *25*, 1149−1157.

(7) (a) Dohmen, C.; Fröhlich, T.; Lächelt, U.; Röhl, I.; Vornlocher, H.-P.; Hadwiger, P.; Wagner, E. *Mol. Ther. Nucleic Acids* **2012**, *1*, e7. (b) Thomas, M.; Kularatne, S. A.; Qi, L. W.; Kleindl, P.; Leamon, C. P.; Hansen, M. J.; Low, P. S. *Ann. N.Y. Acad. Sci.* **2009**, *1175*, 32−39. (c) Zhang, K. X.; Wang, Q. Q.; Xie, Y. H.; Mor, G.; Sega, E.; Low, P. S.; Huang, Y. Q. *RNA* **2008**, *14*, 577−583.

(8) Kortylewski, M.; Swiderski, P.; Herrmann, A.; Wang, L.; Kowolik, C.; Kujawski, M.; Lee, H.; Scuto, A.; Liu, Y.; Yang, C. M.; Deng, J. H.; Soifer, H. S.; Raubitschek, A.; Forman, S.; Rossi, J. J.; Pardoll, D. M.; Jove, R.; Yu, H. *Nat. Biotechnol.* **2009**, *27*, 925−932.

(9) (a) Kim, S. H.; Jeong, J. H.; Lee, S. H.; Kim, S. W.; Park, T. G. *Bioconjugate Chem.* **2008**, *19*, 2156−2162. (b) Rozema, D. B.; Lewis, D. L.; Wakefield, D. H.; Wong, S. C.; Klein, J. J.; Roesch, P. L.; Bertin, S. L.; Reppen, T. W.; Chu, Q.; Blokhin, A. V.; Hagstrom, J. E.; Wolff, J. A. *Proc. Natl. Acad. Sci. U.S.A.* **2007**, *104*, 12982−12987. (c) Derfus, A. M.; Chen, A. A.; Min, D. H.; Ruoslahti, E.; Bhatia, S. N. *Bioconjugate Chem.* **2007**, *18*, 1391−1396. (d) Choi, C. H. J.; Alabi, C. A.; Webster, P.; Davis, M. E. *Proc. Natl. Acad. Sci. U.S.A.* **2010**, *107*, 1235−1240. (e) Zhang, K.; Hao, L.; Hurst, S. J.; Mirkin, C. A. *J. Am. Chem. Soc.* **2012**, *134*, 16488−16491. (f) Lee, J.; Yun, K. S.; Choi, C. S.; Shin, S. H.; Ban, H. S.; Rhim, T.; Lee, S. K.; Lee, K. Y. *Bioconjugate Chem.* **2012**, *23*, 1174−1180. (g) Lee, H.; Lytton-Jean, A. K. R.; Chen, Y.; Love, K. T.; Park, A. I.; Karagiannis, E. D.; Sehgal, A.; Querbes, W.; Zurenko, C. S.; Jayaraman, M.; Peng, C. G.; Charisse, K.; Borodovsky, A.; Manoharan, M.; Donahoe, J. S.; Truelove, J.; Nahrendorf, M.; Langer, R.; Anderson, D. G. *Nat. Nanotechnol.* **2012**, *7*, 389−393. (h) Chen, Y. C.; Zhu, X. D.; Zhang, X. J.; Liu, B.; Huang, L. *Mol. Ther.* **2010**, *18*, 1650−1656. (i) Sato, Y.; Murase, K.; Kato, J.; Kobune, M.; Sato, T.; Kawano, Y.; Takimoto, R.; Takada, K.; Miyanishi, K.; Matsunaga, T.; Takayama, T.; Niitsu, Y. *Nat. Biotechnol.* **2008**, *26*, 431−442. (j) Peer, D.; Park, E. J.; Morishita, Y.; Carman, C. V.; Shimaoka, M. *Science* **2008**, *319*, 627−630.

(10) (a) Shen, B. Q.; Xu, K. Y.; Liu, L. N.; Raab, H.; Bhakta, S.; Kenrick, M.; Parsons-Reponte, K. L.; Tien, J.; Yu, S. F.; Mai, E.; Li, D. W.; Tibbitts, J.; Baudys, J.; Saadi, O. M.; Scales, S. J.; McDonald, P. J.; Hass, P. E.; Eigenbrot, C.; Nguyen, T.; Solis, W. A.; Fuji, R. N.; Flagella, K. M.; Patel, D.; Spencer, S. D.; Khawlil, L. A.; Ebens, A.; Wong, W. L.; Vandlen, R.; Kaur, S.; Sliwkowski, M. X.; Scheller, R. H.; Polakis, P.; Junutula, J. R. *Nat. Biotechnol.* **2012**, *30*, 184−189. (b) Junutula, J. R.; Raab, H.; Clark, S.; Bhakta, S.; Leipold, D. D.; Weir, S.; Chen, Y.; Simpson, M.; Tsai, S. P.; Dennis, M. S.; Lu, Y. M.; Meng, Y. G.; Ng, C.; Yang, J. H.; Lee, C. C.; Duenas, E.; Gorrell, J.; Katta, V.; Kim, A.; McDorman, K.; Flagella, K.; Venook, R.; Ross, S.; Spencer, S. D.; Wong, W. L.; Lowman, H. B.; Vandlen, R.; Sliwkowski, M. X.; Scheller, R. H.; Polakis, P.; Mallet, W. *Nat. Biotechnol.* **2008**, *26*, 925−932. (c) Wu, A. M.; Senter, P. D. *Nat. Biotechnol.* **2005**, *23*, 1137−1146.

(11) (a) Wu, X.; Schultz, P. G. *J. Am. Chem. Soc.* **2009**, *131*, 12497−12515. (b) Wang, L.; Brock, A.; Herberich, B.; Schultz, P. G. *Science* **2001**, *292*, 498−500.

(12) (a) Wang, L.; Zhang, Z. W.; Brock, A.; Schultz, P. G. *Proc. Natl. Acad. Sci. U.S.A.* **2003**, *100*, 56−61. (b) Liu, W. S.; Brock, A.; Chen, S.; Chen, S. B.; Schultz, P. G. *Nat. Methods* **2007**, *4*, 239−244.

(13) (a) Kazane, S. A.; Axup, J. Y.; Kim, C. H.; Ciobanu, M.; Wold, E. D.; Barluenga, S.; Hutchins, B. A.; Schultz, P. G.; Winssinger, N.; Smider, V. V. *J. Am. Chem. Soc.* **2013**, *135*, 340−346. (b) Kazane, S. A.; Sok, D.; Cho, E. H.; Uson, M. L.; Kuhn, P.; Schultz, P. G.; Smider, V. V. *Proc. Natl. Acad. Sci. U.S.A.* **2012**, *109*, 3731−3736. (c) Axup, J. Y.; Bajjuri, K. M.; Ritland, M.; Hutchins, B. M.; Kim, C. H.; Kazane, S. A.; Halder, R.; Forsyth, J. S.; Santidrian, A. F.; Stafin, K.; Lu, Y. C.; Tran,

H.; Seller, A. J.; Biroce, S. L.; Szydlik, A.; Pinkstaff, J. K.; Tian, F.; Sinha, S. C.; Felding-Habermann, B.; Smider, V. V.; Schultz, P. G. *Proc. Natl. Acad. Sci. U.S.A.* **2012**, *109*, 16101−16106. (d) Kim, C. H.; Axup, J. Y.; Dubrovska, A.; Kazane, S. A.; Hutchins, B. A.; Wold, E. D.; Smider, V. V.; Schultz, P. G. *J. Am. Chem. Soc.* **2012**, *134*, 9918−9921.
(14) Ross, J. S.; Slodkowska, E. A.; Symmans, W. F.; Pusztai, L.; Ravdin, P. M.; Hortobagyi, G. N. *Oncologist* **2009**, *14*, 320−368.
(15) Hutchins, B. M.; Kazane, S. A.; Staflin, K.; Forsyth, J. S.; Felding-Habermann, B.; Schultz, P. G.; Smider, V. V. *J. Mol. Biol.* **2011**, *406*, 595−603.
(16) (a) Zhou, P.; Wang, M. M.; Du, L.; Fisher, G. W.; Waggoner, A.; Ly, D. H. *J. Am. Chem. Soc.* **2003**, *125*, 6878−6879. (b) Luedtke, N. W.; Carmichael, P.; Tor, Y. *J. Am. Chem. Soc.* **2003**, *125*, 12374−12375. (c) Wender, P. A.; Mitchell, D. J.; Pattabiraman, K.; Pelkey, E. T.; Steinman, L.; Rothbard, J. B. *Proc. Natl. Acad. Sci. U.S.A.* **2000**, *97*, 13003−13008.